Heavy Flavor and Quarkonium Production and Interactions in Media

R. Vogt

Lawrence Livermore National Laboratory, Livermore, CA 94551, USA
Physics and Astronomy Department, UC Davis, Davis, CA 95616, USA

Figure 1: This work was performed under the auspices of the U.S. Department of Energy by Lawrence Livermore National Laboratory under Contract DE-AC52-07NA27344, the LLNL-LDRD Program under Projects 21-LW-034 and 23-LW-036 and the HEFTY Collaboration.

Many Experimental Programs Study Heavy Flavors

PHENIX and STAR studied open heavy flavor and quarkonium at RHIC, measured nuclear suppression factor R_{AA} and flow v_2 for J/ψ and D mesons up to $\sqrt{s_{NN}} = 200$ GeV, in $p+p$, $p+A$, ($A = \mathrm{He}$, Al, Au), d+Au, Au+Au, U+U

STAR recently separated Υ(1S), Υ(2S) and Υ(3S) states at RHIC; sPHENIX is turning on now and will have better separation of peaks; also plans to study b-jets

LHC experiments have provided a wealth of data on heavy flavor probes, including those at RHIC up to higher p_T as well as heavy flavor jets and $Z + c$-jets; showed hadronization is different for charm baryons and mesons in medium than in vacuum; $p+p$ collisions at $\sqrt{s} = 5.02$, 7, 8 and 13 TeV; $p+\mathrm{Pb}$ at $\sqrt{s_{NN}} = 5.02$ and 8 TeV; Pb+Pb at $\sqrt{s_{NN}} = 2.76$ and 5 TeV

J/ψ and ψ(2S) measurements in ultraperipheral collisions and semi-peripheral collisions probe gluon content of the nucleon and nucleus

LHC experiments also studying exotic hadrons $X(3872)$ and more; LHCb has discovered a plethora of new exotic states, including many potential tetraquark states

LHCb fixed-target studies J/ψ and D mesons at $\sqrt{s_{NN}} = 68.5$, 86.6, and 110.4 GeV in $p + \mathrm{Ne}$, $p + \mathrm{He}$, and $p + \mathrm{Ar}$ collisions respectively; looking for intrinsic charm

Other fixed-target data taken recently or planned: SeaQuest at FNAL, $p_{\mathrm{beam}} = 120$ GeV; COMPASS, NA60+ at CERN SPS, CBM at FAIR; JLab measurement probes gravitational form factor of proton

The EIC will add to heavy-flavor data and theory when it comes on

Open Heavy Flavor Production

Calculating Open Heavy Flavors in Perturbative QCD

Hard processes have a large scale in the calculation that makes perturbative QCD applicable, since $m \neq 0$, heavy quark production is a hard process

Total cross section **in a pp collision, assuming collinear factorization**

$$\sigma_{pp}(s, m^2) \;=\; \sum_{i,j=q,\overline{q},g} \int_{4m_Q^2/s}^{1} \frac{d\tau}{\tau} \int dx_1\, dx_2\, \delta(x_1 x_2 - \tau) f_i^p(x_1, \mu_F^2)\, f_j^p(x_2, \mu_F^2)\, \widehat{\sigma}_{ij}(\hat{s}, m^2, \mu_F^2, \mu_R^2)$$

f_i^A are nonperturbative parton distributions, determined from global analyses of data sets over many scales, x_1, x_2 are proton momentum fractions carried by partons i and j, $\tau = \hat{s}/s$

$\widehat{\sigma}_{ij}(\hat{s}, m^2, \mu_F^2, \mu_R^2)$ is hard partonic cross section calculable in QCD in powers of α_s^{2+n}: leading order (LO), $n = 0$; next-to-leading order (NLO), $n = 1$ ...

Schematic *single inclusive* heavy flavor production

$$E\frac{d^3\sigma_{\rm fs}}{d^3p} = E_Q \frac{d^3\sigma_Q}{d^3p_Q} \otimes D(Q \to H_Q) \otimes f(H_Q \to {\rm fs})$$

Results depend strongly on quark mass, m, factorization scale, μ_F, in the parton densities and renormalization scale, μ_R, in α_s

FONLL and ZM-VFN schemes treat heavy quark as light for large p_T/m logs at high p_T, match massive and massless parts

Examples of Single Inclusive Calculations

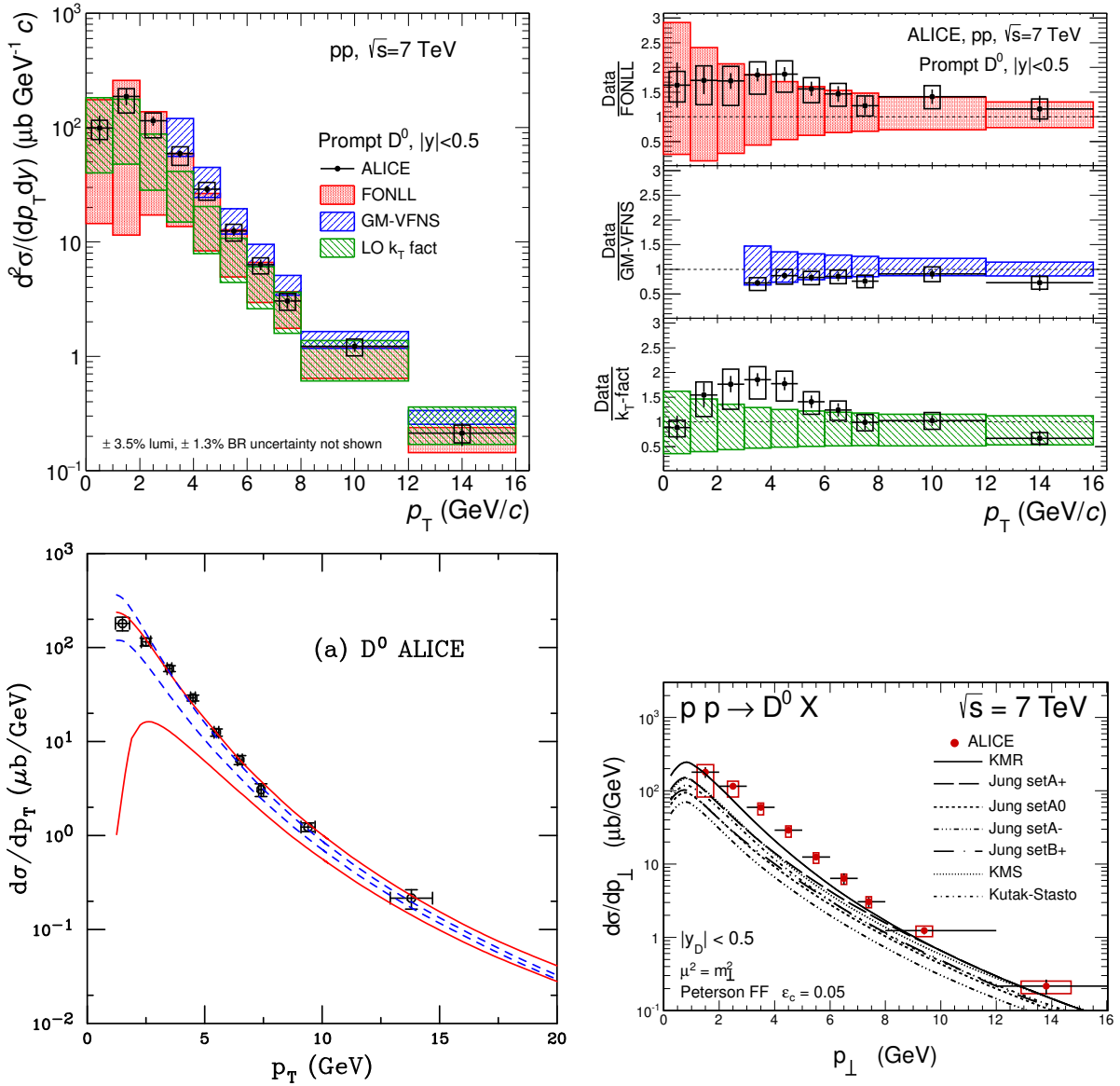

Figure 2: **(Top) ALICE Collaboration, Phys. Rev. C 94 (2016) 05490. (Bottom left) Nelson, Frawley and RV (Bottom right) Maciula and Szczurek**

Correlated $Q\overline{Q}$ Pair Production

Exclusive calculations needed for correlations, retains all $Q\overline{Q}$ kinematic quantities

Calculational approaches to $Q\overline{Q}$ production:

- **HVQMNR (Mangano, Nason and Ridolfi): no resummation, negative weight MC, incomplete numerical cancellation of divergences at $p_T \to 0$; adding k_T broadening is a proxy for resummation; Peterson function is default fragmentation scheme, fragmentation parameter can be varied**
- **POWHEG-hvq (Frixione, Nason and Ridolfi): leading log resummation, positive weight MC, generally interfaces with parton shower LO MC like HERWIG or PYTHIA for fragmentation and decay**
- **LO event generators like PYTHIA: events are not grouped according to initial state like gg, $q\overline{q}$, and $q(\overline{q})g$ as in pQCD but according to topology (flavor creation, flavor excitation and gluon splitting)**

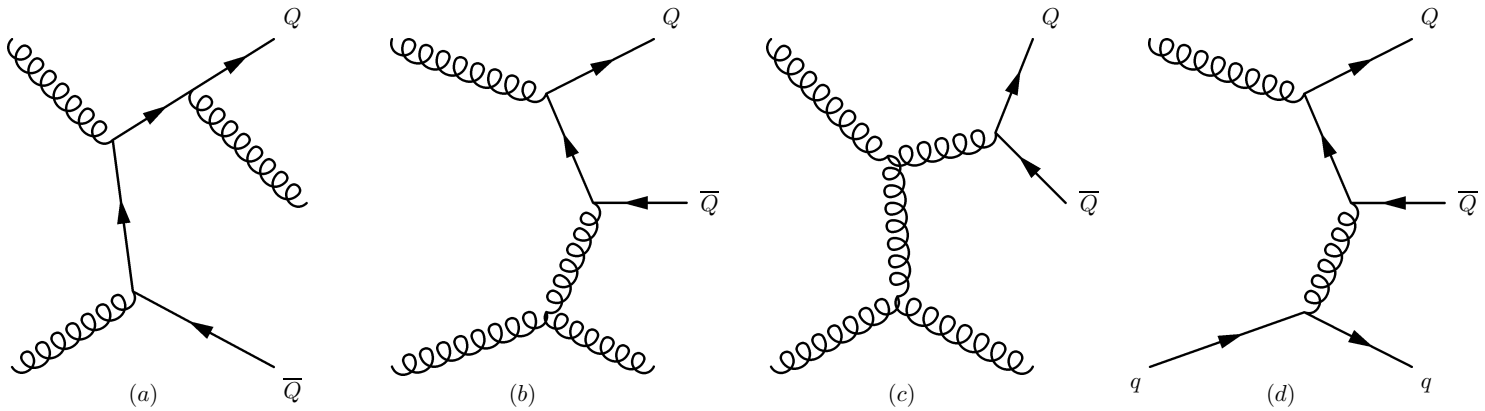

Figure 3: Examples of real contributions to next-to-leading order $Q\overline{Q}$ production. Diagrams (a)-(c) illustrate contributions to $gg \to Q\overline{Q}g$ while (d) shows an example of $qg \to qQ\overline{Q}$ production.

LHCb Measured Charm Pair Correlations

Measured cc (D^+D^+) and $c\bar{c}$ (D^+D^-) pairs

10 times more $c\bar{c}$ events than cc (more isotropic in $\Delta\phi$ and harder pair p_T distributions)

cc events likely due to double parton scattering while $c\bar{c}$ events arise from single parton scattering

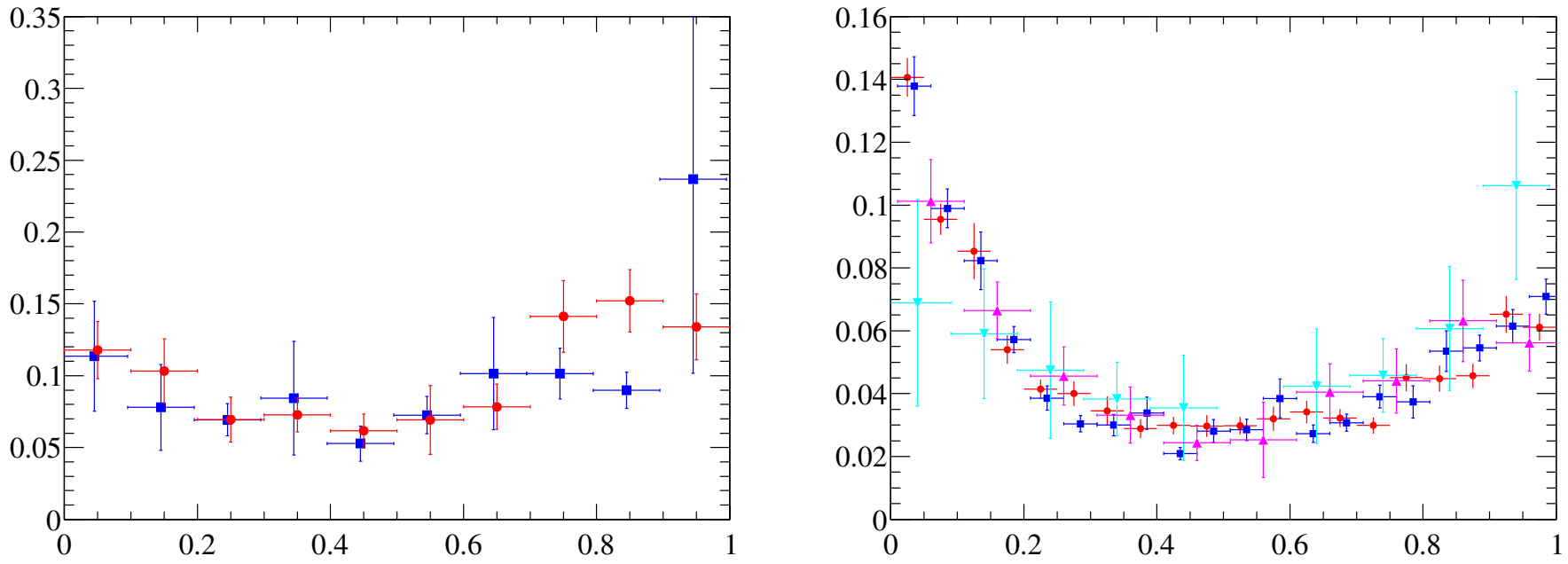

Figure 4: **(Left)** cc $\Delta\phi/\pi$. **(Right)** $c\bar{c}$ $\Delta\phi/\pi$. **Both measured at $\sqrt{s} = 7$ TeV by LHCb [R. Aaij *et al.* [LHCb Collaboration], JHEP 1206, 141 (2012), [JHEP 1403, 108 (2014)]].**

Charm $\Delta\phi$ Distributions Compared to CDF and LHCb

CDF (Left: $p_T > 5.5$ GeV for D^0, D^{*-} and 7 GeV for D^+); LHCb (Right: $p_T > 3$ GeV for $D\overline{D}$ pairs)

Δ is a measure of k_T kick, a larger kick makes $|\Delta\phi|$ more isotropic, especially at low p_T, at higher charm p_T there is still a back-to-back peak as well

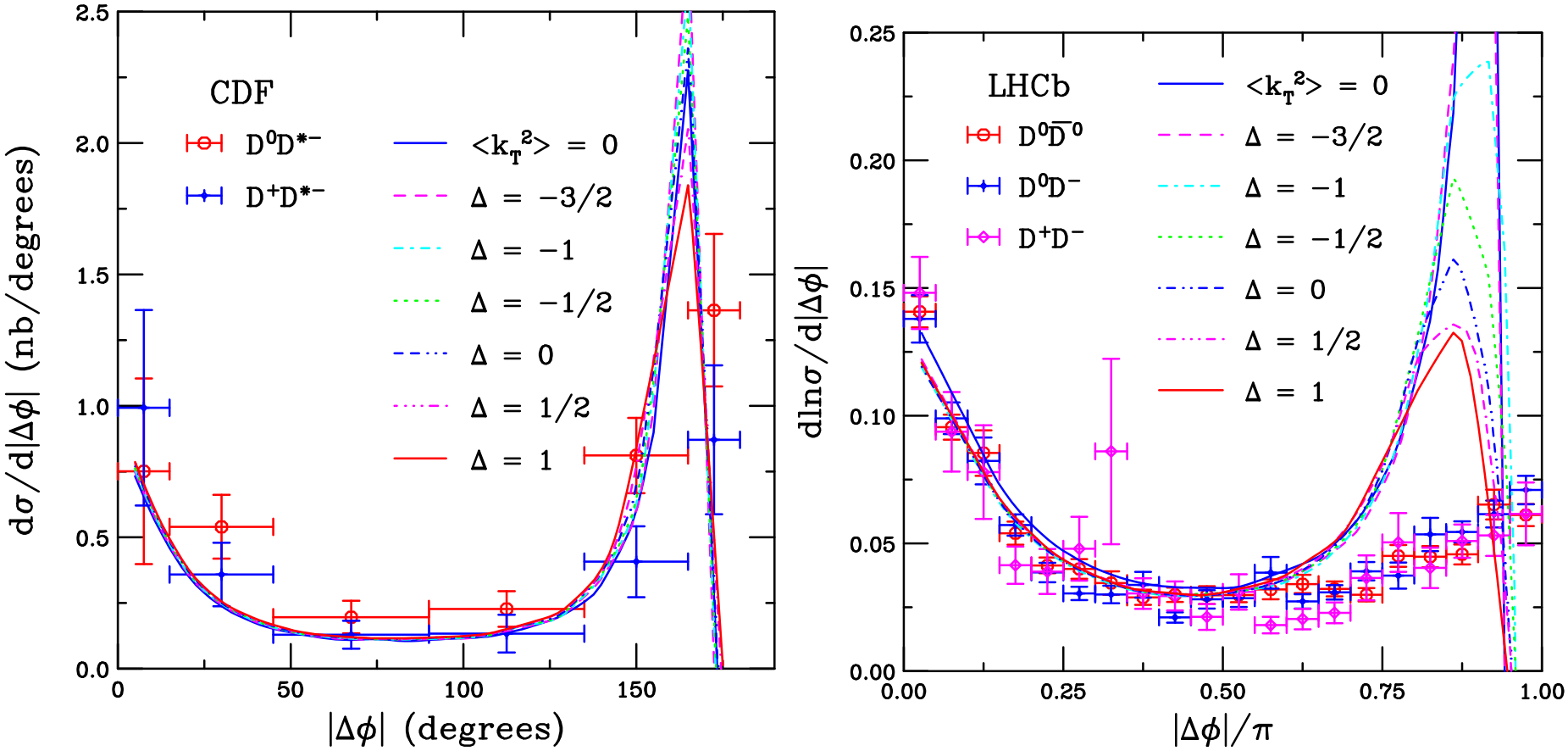

Figure 5: **(Left) The azimuthal angle distributions for D^0D^{*-} (red) and D^+D^{*-} (blue) pairs measured in $p+\overline{p}$ collisions at $\sqrt{s} = 1.96$ TeV by CDF [B. Reisert *et al.* [CDF Collaboration], Nucl. Phys. Proc. Suppl. 170, 243 (2007)]. The data are compared to calculations in the same acceptance with $\langle k_T^2 \rangle = 0$ and for values of Δ from $-3/2$ to 1. (Right) The azimuthal angle distributions for $D^0\overline{D}^0$ (red), D^0D^- (blue), and D^+D^- (magenta) pairs measured in $p+p$ collisions at $\sqrt{s} = 7$ TeV by LHCb [R. Aaij *et al.* [LHCb Collaboration], JHEP 1206, 141 (2012), [JHEP 1403, 108 (2014)]] The data are compared to calculations in the same acceptance with $\langle k_T^2 \rangle = 0$ and for values of Δ from $-3/2$ to 1.**

Distributions $|\Delta\phi^*|$ and $|\Delta\phi|$ between $J/\psi J/\psi$ and $b\bar{b}$

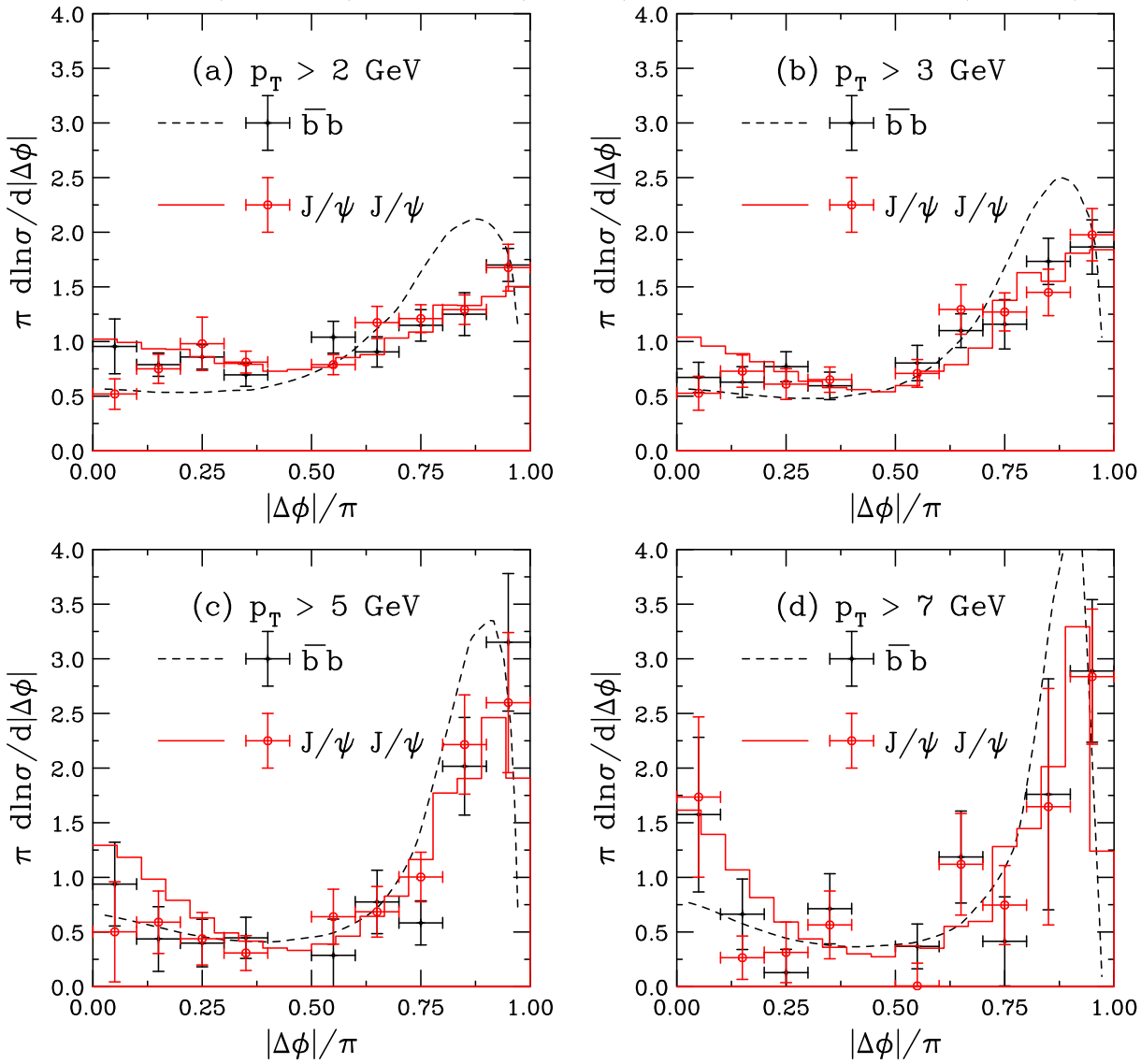

Figure 6: **The azimuthal angle difference between the b and $\overline{b}$ (black dashed curves) and the J/ψ's resulting from B decays (red histograms) are compared to the LHCb data (black: $b\bar{b}$, red circles: J/ψ pairs) for p_T cuts on the B and the J/ψ of 2 (a), 3 (b), 5 (c) and 7 GeV (d). Measurement from LHCb, JHEP 11, 030 (2017).**

Quarkonium Production

Quarkonium Production Approaches

Color Singlet Model (CSM):

$\mathcal{O}(m_Q)$, **singlet states produced with correct quantum numbers; hard gluon needed for** S **state production,** *e.g.* $gg \to J/\psi g$; $gg \to \chi_{c2}$ **is direct singlet (Baier** *et al.*; **Schuler)**

(Improved) Color Evaporation Model ((I)CEM):

$\mathcal{O}(\Lambda_{\rm QCD})$, $Q\overline{Q}$ **quantum numbers changed by soft interactions with probabilities specific to each state but independent of energy (Barger** *et al.*; **Gavai** *et al.*; **Schuler and RV); improved by making mass cut and momentum scale depend on quarkonium state produced (Ma and RV); further improved by introducing polarization; introducing other processes beyond hadroproduction (Cheung and RV, both** k_T **and collinear factorization studied)**

Nonrelativistic QCD (NRQCD):

$\mathcal{O}(\alpha_s m_Q)$, **expansion in** α_s **and relative** $Q\overline{Q}$ **velocity** v, **quantum numbers changed via gluon emission at bound state momentum scale; nonperturbative LDMEs fit to data by various groups but depends strongly on minimum** p_T **scale and which processes are included in fits, including polarization; saturation + NRQCD can solve some low** p_T **issues, as well as polarization, but at sufficiently high energies and with some matching issues at intermediate** p_T**– widely used but questions still remain**

CEM and ICEM Calculations of J/ψ and Υ(1S)

Polarized J/ψ production was studied for the first time in the ICEM

Calculations agree well with measured p_T distributions

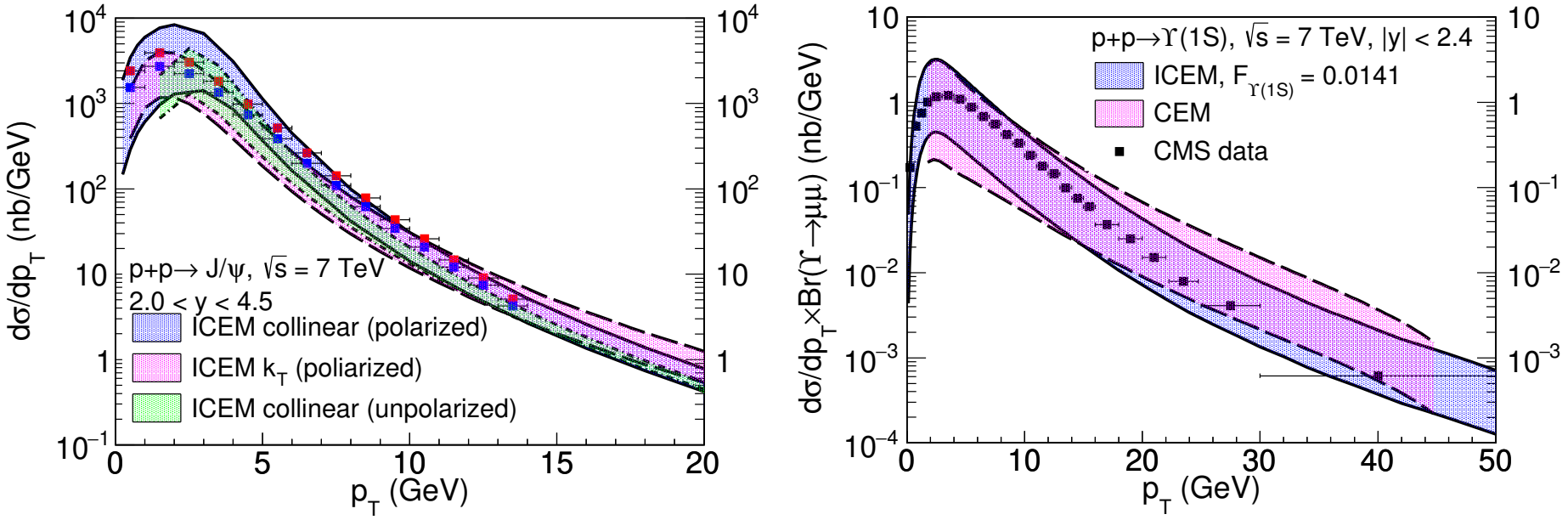

Figure 7: **(Left) The p_T dependence of inclusive J/ψ production at $\sqrt{s} = 7$ TeV in the polarized collinear ICEM (blue region), in the polarized ICEM using k_T factorization (magenta region), and in the unpolarized collinear ICEM (green region). They are compared to the LHCb data (EPJ C 71, 1645 (2011)) assuming that the J/ψ polarization is totally transverse, $\lambda_\theta = +1$ (red squares), and totally longitudinal, $\lambda_\theta = 1$ (blue squares). The LHCb data assuming $\lambda_\theta = 0$ lie between the red and blue points and are not shown. From PRD 104, 094026 (2021). (Right) The p_T dependence of prompt Υ(1S) production at $\sqrt{s} = 7$ TeV in the ICEM with combined mass and renormalization scale uncertainties (blue) and that in the CEM using collinear factorizationx (magenta). The CMS midrapidity data (PLB 727, 101 (2013)) are also shown. From PRD 59, 034007 (2019).**

Polarization Studied in $p+p$ and Pb+Pb Collisions

J/ψ polarization measured in $p+p$ collisions at $\sqrt{s}=7$ TeV and Pb+Pb collisions at $\sqrt{s_{NN}}=5$ TeV

No significant difference seen between p+p and Pb+Pb data or in ICEM calculations assuming no hot matter effects

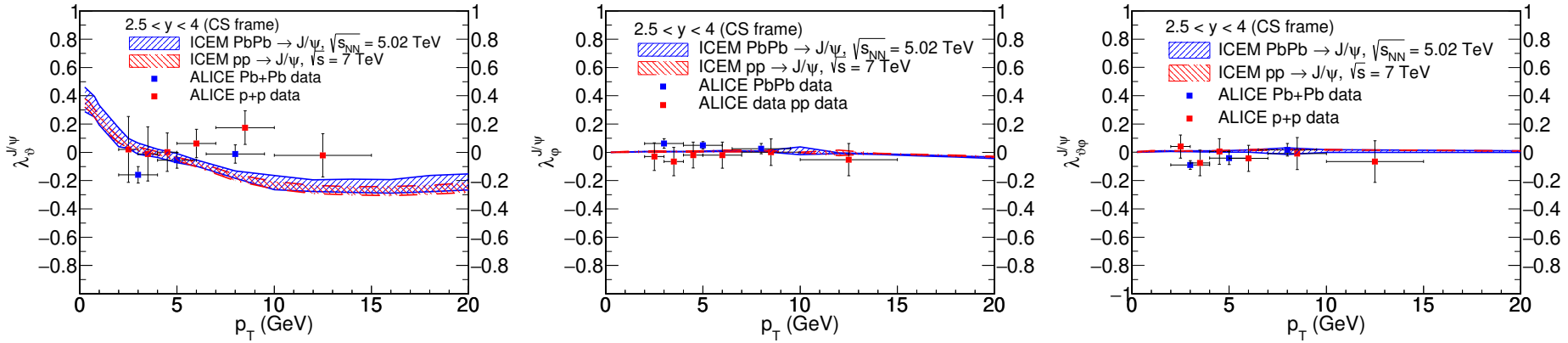

Figure 8: **(a) The polar anisotropy parameter (λ_ϑ), (b) the azimuthal anisotropy parameter (λ_φ), and (c) the polar-azimuthal correlation parameter ($\lambda_{\vartheta\varphi}$) in the Collins-Soper frame in the ICEM. The combined mass, renormalizaton scale, and factorization scale uncertainties are shown in the band and compared to the ALICE Pb+Pb data at $\sqrt{s_{NN}}=5.02$ TeV (PLB 815, 136146 (2021)) (blue) and the ALICE $p+p$ data at $\sqrt{s}=7$ TeV (PRL 108, 082001 (2012)) (red). From PRC 105, 055202 (2022).**

J/ψ Photoproduction in $e + p$ Collisions

V. Cheung and RV, submitted to PRD

First photoproduction calculation in the ICEM, including polarization

Calculations performed at low Q^2 and compared to polarized and unpolarized HERA photoproduction data [Eur. Phys. J. C 68, 401 (2010)]

Top plots: unpolarized production; bottom plots: polarized – polar (left) and azimuthal (right) asymmetries in the helicity (HX) frame

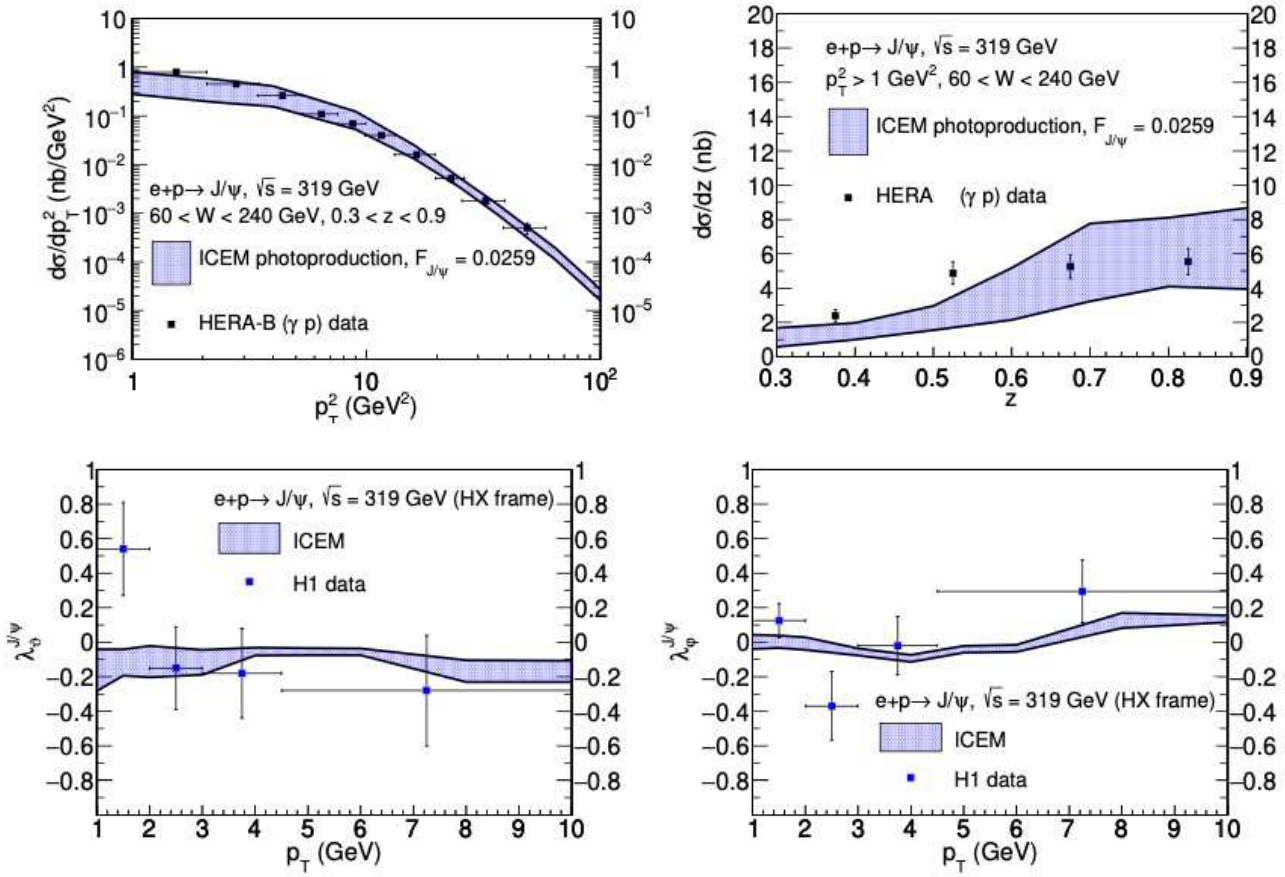

Heavy Flavor Production in Cold Nuclear Matter

Baseline $p+p$ Production in Perturbative QCD

The perturbative QCD cross section at NLO for open heavy flavor and quarkonium is

$$\sigma_{\rm OHF}(pp) \;=\; \sum_{i,j}\int_{4m^2}^{\infty} d\hat{s}\int dx_1\,dx_2\;\; F_i^p(x_1,\mu_F^2,k_{T_1})\;\; F_j^p(x_2,\mu_F^2,k_{T_2})\;\; \hat{\sigma}_{ij}(\hat{s},\mu_F^2,\mu_R^2)\;,$$

$$\sigma_{\rm CEM}(pp) \;=\; F_C\sum_{i,j}\int_{4m^2}^{4m_H^2} ds\int dx_1\,dx_2\;\; F_i^p(x_1,\mu_F^2,k_{T_1})\;\; F_j^p(x_2,\mu_F^2,k_{T_2})\;\; \hat{\sigma}_{ij}(\hat{s},\mu_F^2,\mu_R^2)$$

Parton densities factorized into longitudinal and a k_T-dependent component to implement k_T broadening a la low p_T resummation; Peterson fragmentation with parameter modified to agree with FONLL included for open charm

$$F^p(x,\mu_F^2,k_T) = f^p(x,\mu_F^2)G_p(k_T)$$

$$G_p(k_T) \;=\; \frac{1}{\pi\langle k_T^2\rangle_p}\exp(-k_T^2/\langle k_T^2\rangle_p)$$

$$\langle k_T^2\rangle_p = \left[1+\frac{\Delta}{n}\ln\left(\frac{\sqrt{s_{NN}}(\mathrm{GeV})}{20\,\mathrm{GeV}}\right)\right]\;\mathrm{GeV}^2$$

$\langle k_T^2\rangle_p$ broadening assumed energy dependent, $n=12$ from J/ψ data; 3 for Υ

$\Delta = 1$ for default to study broadening in $p+p$ collisions

Cold Matter Effects on Perturbative Cross Section

Production cross section in a pA collision is

$$\sigma_{pA} = \sigma_{\rm CEM}(pA) = S_A^{\rm abs} F_C \sum_{i,j} \int_{4m^2}^{4m_H^2} ds \int dx_1\, dx_2\ F_i^p(x_1, \mu_F^2, k_T)\ F_j^A(x_2, \mu_F^2, k_T)\ \hat{\sigma}_{ij}(\hat{s}, \mu_F^2, \mu_R^2)$$

Survival probability for absorption of a (proto)charmonium state in nuclear matter:

$$\begin{aligned}\sigma_{pA} = \sigma_{pN} S_A^{\rm abs} &= \sigma_{pN} \int d^2b \int_{-\infty}^{\infty} dz\, \rho_A(b,z) S^{\rm abs}(b) \\ &= \sigma_{pN} \int d^2b \int_{-\infty}^{\infty} dz\, \rho_A(b,z) \exp\left\{ - \int_z^{\infty} dz' \rho_A(b,z') \sigma_{\rm abs}(z'-z) \right\}\end{aligned}$$

The absorption cross section is assumed constant. Prior fixed-target experiments extracted an effective absorption cross section from A^α analysis with $\alpha = 1 - 9\sigma_{\rm abs}/(16\pi r_0^2)$ assuming no other nuclear effects (J/ψ only)

Nuclear parton densities

$$\begin{aligned} F_j^A(x_2, \mu_F^2, k_T) &= R_j(x_2, \mu_F^2, A) f_j(x_2, \mu_F^2) G_A(k_T) \\ F_i^p(x_1, \mu_F^2, k_T) &= f_i(x_1, \mu_F^2) G_p(k_T) \end{aligned}$$

$G_A(k_T)$ includes increased broadening in the nuclear target ($A > 2$)

k_T Broadening in Nuclei

k_T broadening in nuclei may be enhanced through multiple scattering in the target; to implement enhanced broadening, a larger value of $\langle k_T^2 \rangle$ is used for nuclear targets

$$\langle k_T^2 \rangle_A = \langle k_T^2 \rangle_p + \delta k_T^2$$

δk_T^2 gives strength of broadening

$$\delta k_T^2 = (\langle \nu \rangle - 1)\Delta^2(\mu)$$

The broadening strength depends on the interaction scale:

$$\Delta^2(\mu) = 0.225 \frac{\ln^2(\mu/\mathrm{GeV})}{1 + \ln(\mu/\mathrm{GeV})} \mathrm{GeV}^2 \qquad \mu = 2m_c$$

Strength also depends on number of scatterings proton undergoes passing through nuclear target, $\langle \nu \rangle - 1$

$$\langle \nu \rangle = \sigma_{pp}^{\mathrm{in}} \frac{\int d^2b T_A^2(b)}{\int d^2b T_A(b)} = \frac{3}{2} \rho_0 R_A \sigma_{pp}^{\mathrm{in}}$$

T_A is the nuclear profile function, here $\rho_0 = 0.16/\mathrm{fm}^3$, $R_A = 1.2A^{1/3}$, and $\sigma_{pp}^{\mathrm{in}}$ is the inelastic $p + p$ cross section

Nuclear Modification of the Parton Densities

EPPS16 nuclear parton density modifications differentiate between u and d valence quarks and all sea quarks; 20 parameters give 40 error sets + 1 central set

Uncertainties are determined by calculating cross section for each A with all error sets, adding differences around central set for each parameter in quadrature

Lower energies probe higher x, for $0 < y < 1$, the momentum fraction in the nucleus is in the antishadowing and EMC regions (see right-hand plot)

$$f_j^A(x_2, \mu_F^2) = R_j(x_2, \mu_F^2, A) f_j^p(x_2, \mu_F^2)$$

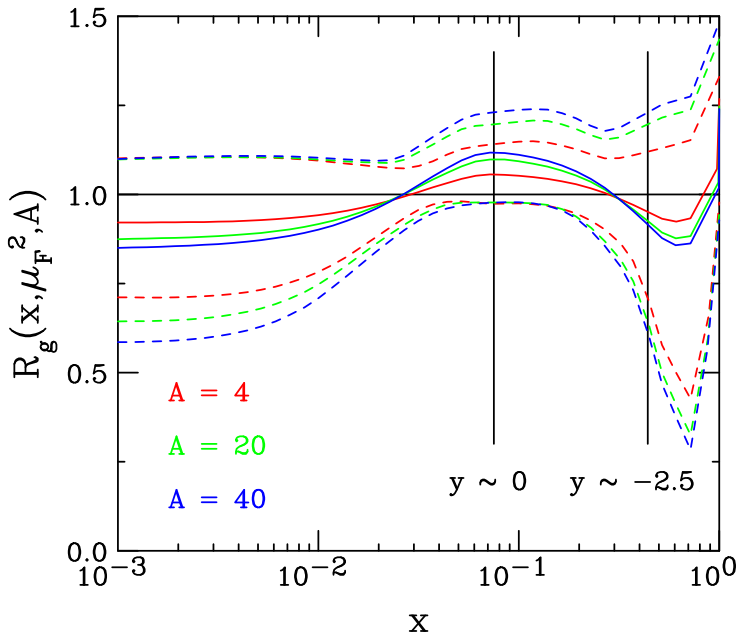

Figure 9: (Color online) The EPPS16 ratios, with uncertainties, are shown at the scale of the J/ψ mass for gluons as a function of momentum fraction x. The central set is denoted by the solid curves while the dashed curves give the upper and lower limits of the uncertainty bands. The results are given for $A = 4$ (red), 20 (green), and 40 (blue). The vertical lines indicate the x range of the SMOG device, $0.075 < x < 0.44$.

Energy Dependence of $\sigma_{\rm abs}^{J/\psi}$

At midrapidity, systematic decrease of $\sigma_{\rm abs}^{J/\psi}$ with $\sqrt{s_{NN}}$, independent of shadowing, trend continues at RHIC and above

$\sigma_{\rm abs}^{J/\psi}(y_{\rm cms}=0)$ at 158 GeV is significantly larger than that measured at 450 GeV

In the antishadowing region, a larger absorption cross section is needed to obtain an overall suppression at fixed-target energies

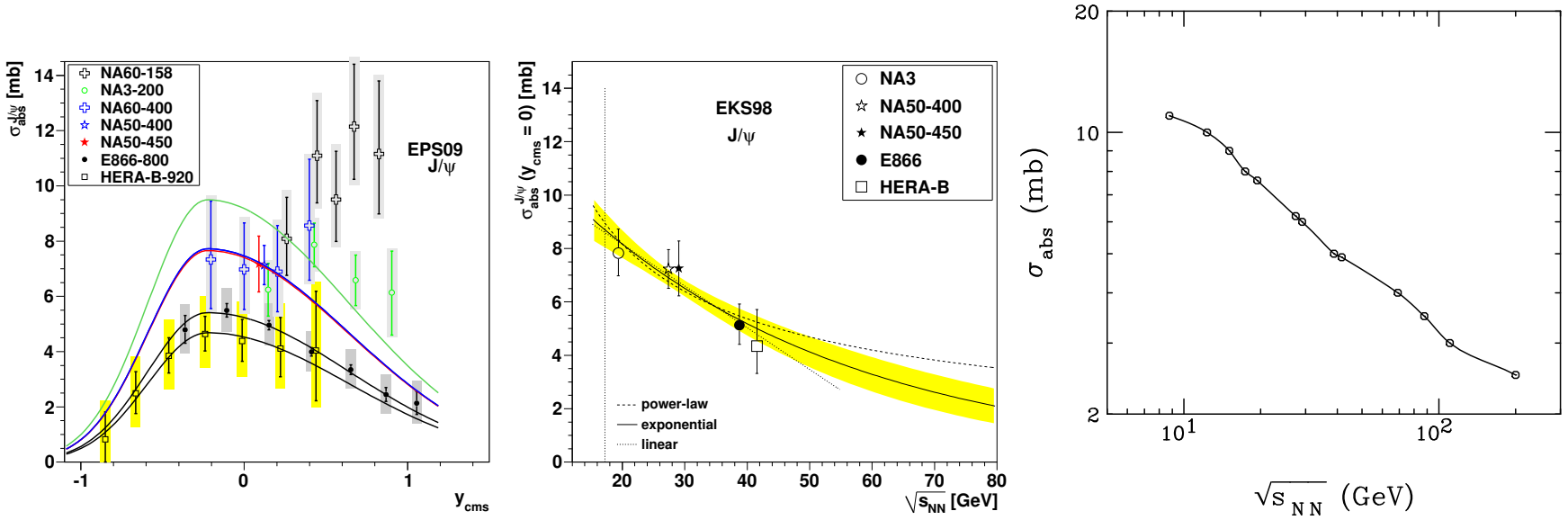

Figure 10: Left: Dependence of $\sigma_{\rm abs}^{J/\psi}$ on $y_{\rm cms}$ for all available data sets including EPS09 shadowing. The shape of the curves is fixed by the E866 and HERA-B data. [Lourenço, RV, Wöhri] Middle: The extracted energy dependence of $\sigma_{\rm abs}^{J/\psi}$ at midrapidity for power law (dashed), exponential (solid) and linear (dotted) approximations to $\sigma_{\rm abs}^{J/\psi}(y=0,\sqrt{s_{NN}})$ using the EKS98 shadowing parameterization with the CTEQ61L parton densities. The band around the exponential curve indicates the uncertainty in the extracted cross sections at $x_F \sim 0$ from NA3, NA50 at 400 and 450 GeV, E866 and HERA-B. The vertical dotted line indicates the energy of the Pb+Pb and In+In collisions at the CERN SPS. [Lourenço, RV, Wöhri] Right: The value of $\sigma_{\rm abs}$ as a function of $\sqrt{s_{NN}}$. The points show the energies used here. The line is meant to guide the eye.

Bottomonium suppression in 5.02 and 8.16 TeV $p+\mathrm{Pb}$ collisions

M, Strickland, S. Thapa and RV, arXiv:2401.16704 (Phys. Rev. D 109, 096016 (2024))

Comprehensive look at Υ suppression in cold (+ hot) matter

- **nPDF effects included with EPPS21, calculated in the color evaporation model with intrinsic k_T broadening in $p+p$ collisions**
- **Energy loss and momentum broadening in media included (Arleo and Peigne)**
  - **Coherent energy loss with quenching parameter $\hat{q}$**
  - **Transverse momentum broadening in medium, $\delta p_T = (\ell_A^2 - \ell_p^2)^{1/2}$ with $\ell_A^2 = \hat{q} L_A$**
- **NLO pNRQCD + Open Quantum Systems (hot matter)**
  - **Lindblad equation including singlet-octet, octet-singlet and octet-octet transitions**
  - **3+1D anisotropic hydrodynamic background**
  - **Temperature dependence of hydro enables differences in suppression between $\Upsilon(n\mathrm{S})$ states**
- **Excited state feed down as in PRD 108, 094024 (2023)**

$$R_{pA}^{\Upsilon} = R_{pA}^{\mathrm{EPPS21}} \times R_{pA}^{\mathrm{eloss},\delta p_T} \times R_{pA}^{\mathrm{HNM}}$$

Comparison to LHC Data

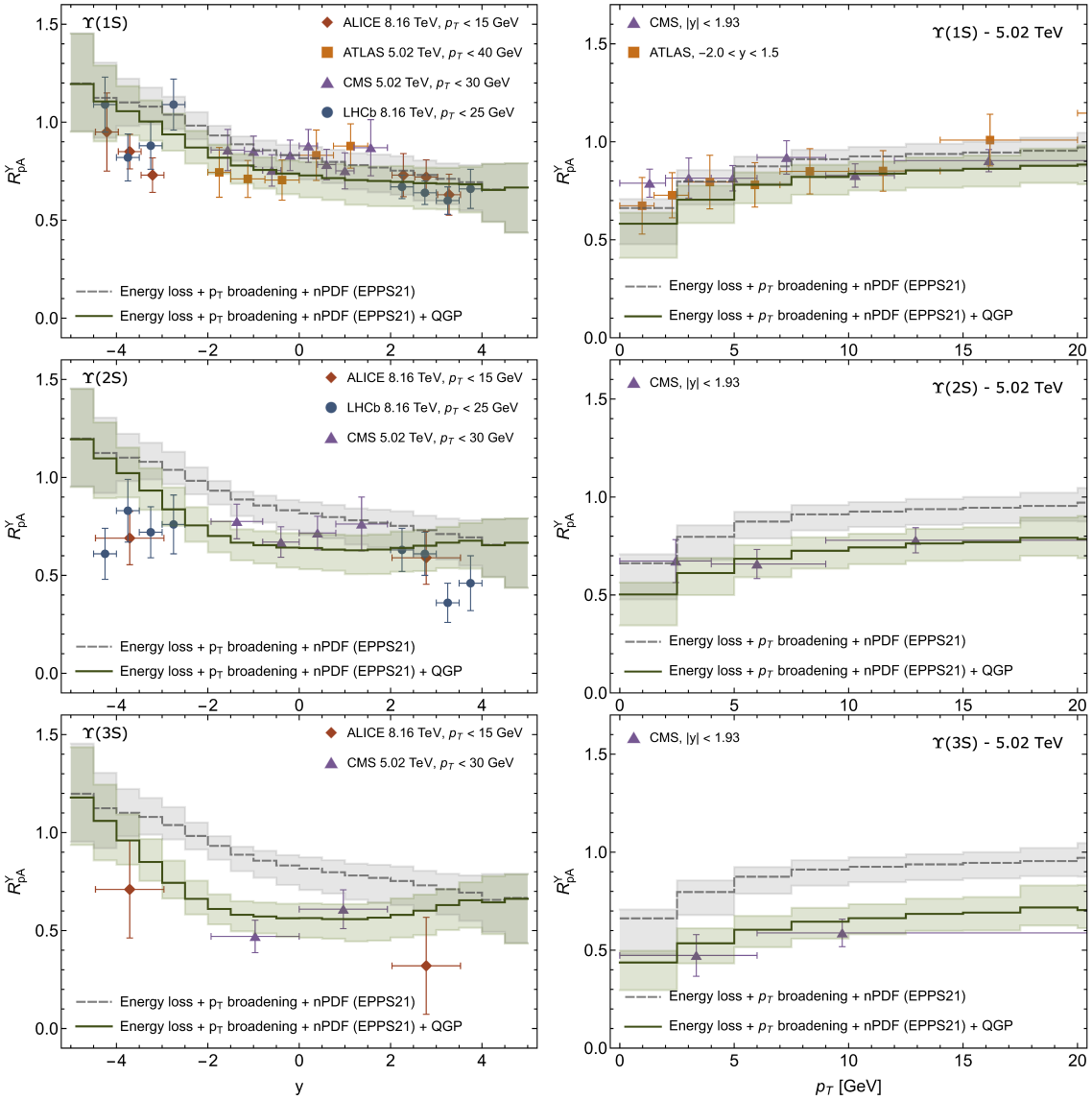

Heavy Flavor Production by Intrinsic Charm

What is Intrinsic Charm?

Proton wavefunction can be expanded as sum over complete basis of quark and gluon states: $|\Psi_p\rangle = \sum_m |m\rangle\, \psi_{m/p}(x_i, k_{T,i}, \lambda_i)$

$|m\rangle$ **are color singlet state fluctuations into Fock components** $|uud\rangle$, $|uudg\rangle \cdots |uudc\overline{c}\rangle$

The intrinsic charm fluctuations can be freed by a soft interaction if the system is probed during the time $\Delta t = 2p_{\rm lab}/M^2_{c\overline{c}}$ **that the fluctuations exist**

Dominant Fock state configurations have minimal invariant mass, $M^2 = \sum_i m^2_{T,i}/x_i$, **where** $m^2_{T,i} = k^2_{T,i} + m^2_i$ **is the squared transverse mass of parton** i **in the state; corresponds to configurations with equal rapidity constituents**

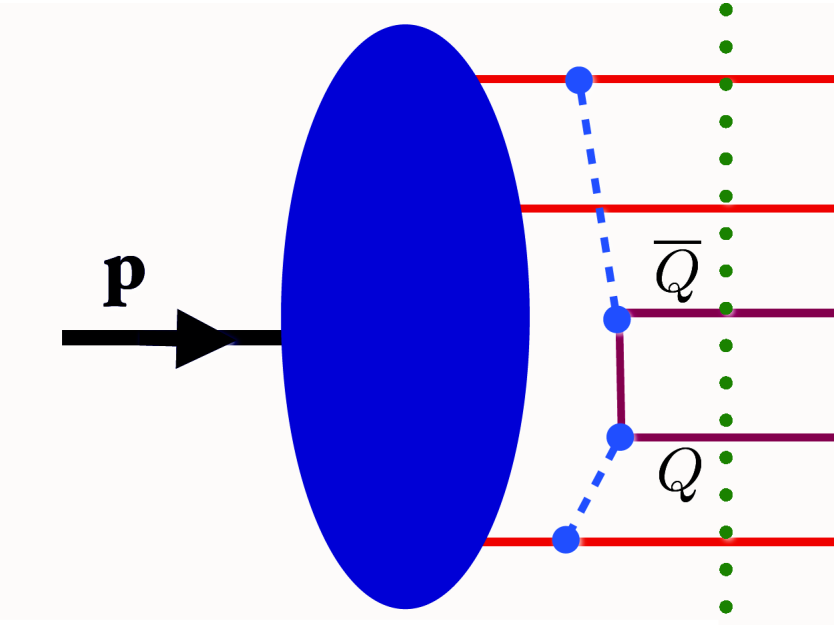

Intrinsic Charm is a Long-Standing Puzzle in QCD

Intrinsic charm in the proton $|uudc\bar{c}\rangle$, was first proposed in the 1980's

If this state dominates the wavefunction, the charm quarks carry a larger fraction of the hadron momentum, enhancing charm production in the forward x_F region

A number of experimental hints have been seen, no conclusive results

- **Charm structure function, F_2^c, large at largest x and highest Q^2 measured (EMC)**
- **Leading charm asymmetries consistent with intrinsic charm predictions (D^- over D^+ in $\pi^- p$ interactions, E791)**
- **Double J/ψ production observed at high pair x_F by NA3**
- **Forward charm production observed in many fixed-target experiments (WA82, WA89, E791, SELEX and others)**
- **Proposed explanation of high energy astrophysical neutrino rate at Ice Cube (Brodsky and Laha)**
- **LHCb Z+c-jet measurements at forward rapidity consistent with intrinsic charm**

Global PDF analyses have tried incorporating intrinsic charm and reported a range of possible contributions from 0 to 1%, most lately the NNPDF Collaboration (Nature) and the CTEQ Collaboration

At colliders, intrinsic charm is boosted to high rapidity and detection is less likely, fixed-target configurations may be better for discovery measurement

Heavy Flavor Production by Intrinsic Charm

Probability distribution of five-particle Fock state of the proton:

$$dP_{\mathrm{ic}\,5} = P^0_{\mathrm{ic}\,5} N_5 \int dx_1 \cdots dx_5 \int dk_{x\,1} \cdots dk_{x\,5} \int dk_{y\,1} \cdots dk_{y\,5} \frac{\delta(1-\sum_{i=1}^5 x_i)\delta(\sum_{i=1}^5 k_{x\,i})\delta(\sum_{i=1}^5 k_{y\,i})}{(m_p^2 - \sum_{i=1}^5 (\widehat{m}_i^2/x_i))^2}$$

$i = 1, 2, 3$ are u, u, d light quarks, 4 and 5 are c and $\overline{c}$, N_t normalizes the probability to unity and P^0_{ic} scales the normalized probability to the assumed intrinsic charm content: 0.1%, 0.31% and 1% are used to represent the range of probabilities assumed previously (based on original Brodsky *et al.* model

The IC cross section is determined from soft interaction scale breaking coherence of the Fock state, $\mu^2 = 0.1$ GeV^2

$$\sigma_{\mathrm{ic}}(pp) = P_{\mathrm{ic}\,5} \sigma^{\mathrm{in}}_{pN} \frac{\mu^2}{4\widehat{m}_c^2}$$

The cross sections from intrinsic charm are then obtained by multiplying by the normalization factor for the CEM to the J/ψ while we assume direct correspondence with IC cross section for $\overline{D}^0$

$$\sigma^{\overline{D}}_{\mathrm{ic}}(pp) = \sigma_{\mathrm{ic}}(pp) \quad , \sigma^{J/\psi}_{\mathrm{ic}}(pp) = F_C \sigma_{\mathrm{ic}}(pp)$$

The A dependence is the same for both $\overline{D}$ and J/ψ

$$\sigma_{\mathrm{ic}}(pA) = \sigma_{\mathrm{ic}}(pp)\, A^\beta \quad , \beta = 0.71 \ \ (\mathrm{NA3})$$

Other assumptions of intrinsic charm distributions in the nucleon are the meson cloud model ($c(x) \neq \overline{c}(x)$) and a sea-like distribution ($c(x) = \overline{c}(x) \propto \overline{d}(x) + \overline{u}(x)$)

Combining Perturbative and Nonperturbative (Intrinsic) Charm

J/ψ and D meson production included

The production cross sections are calculated with a combination of perturbative QCD and intrinsic charm contributions; in $p+p$ collisions:

$$\begin{aligned} \sigma_{pp}^{\overline{D}} &= \sigma_{\rm OHF}(pp) + \sigma_{\rm ic}^{\overline{D}}(pp) \\ \sigma_{pp}^{J/\psi} &= \sigma_{\rm CEM}(pp) + \sigma_{\rm ic}^{J/\psi}(pp) \end{aligned}$$

The D meson and J/ψ cross sections are computed at NLO in the color evaporation model for $p+p$ and $p+A$ interactions; $\sigma_{\rm ic}$ is the intrinsic charm cross section using Brodsky *et al.* "flavor" of IC

In $p+A$ collisions:

$$\begin{aligned} \sigma_{pA}^{\overline{D}} &= \sigma_{\rm OHF}(pA) + \sigma_{\rm ic}^{\overline{D}}(pA) \\ \sigma_{pA}^{J/\psi} &= \sigma_{\rm CEM}(pA) + \sigma_{\rm ic}^{J/\psi}(pA) \end{aligned}$$

Recent and Forthcoming Fixed-Target Experiments Ideal for IC Studies

Many previous experiments studied J/ψ production off nuclear targets at proton beam energies from 158 to 920 GeV, several used to get a baseline for $A + A$ collisions; those that covered large x_F saw a larger suppression of production off nuclear targets at higher x_F

SeaQuest: Took data with a 120 GeV proton beam on p, d, C, Fe, and W targets, covered forward region, $0.4 < x_F < 0.95$ and $p_T < 2.3$ GeV; J/ψ data not published yet but should report nuclear suppression factor, $pA/p\mathrm{d}$

SMOG: Gas jet target in LHCb, J/ψ and D^0 measured at backward rapidity in the fixed-target center of mass, data so far at: $p + \mathrm{Ne}$ at $\sqrt{s_{NN}} = 68.5$ GeV; $p + \mathrm{He}$ at $\sqrt{s_{NN}} = 86.6$ GeV; and $p + \mathrm{Ar}$ at $\sqrt{s_{NN}} = 110.4$ GeV

NA60+: proton beams at $p_{\mathrm{lab}} = 40$, 80, and 120 GeV, nuclear targets from Be to Pb

Calculations and comparison to data in the following from R. Vogt, arXiv:2101.02858, Phys. Rev. C 103, 035204 (2021); arXiv:2207.04347, Phys. Rev. C 106, 025201 (2022); arXiv:2304.03451, Phys. Rev. C 108, 015201 (2023)

SMOG $\overline{D}^0$ Results Compared to Calculations

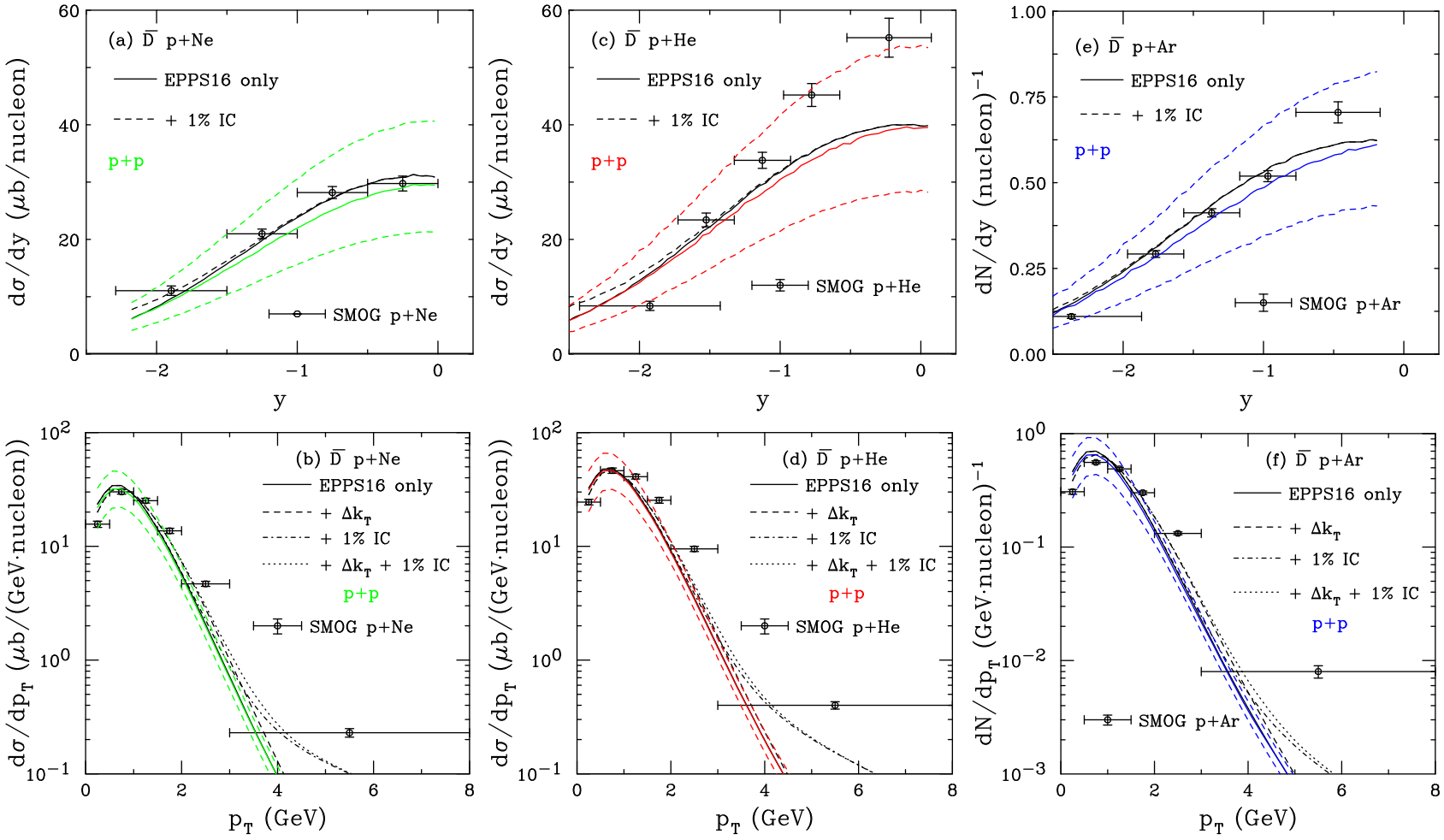

Figure 11: The $\overline{D}$ cross section as a function of y in (a), (c), (e) and p_T in (b), (d), (f) for $p+$Ne ($\sqrt{s_{NN}} = 68.5$ GeV) in (a) and (b); $p+$He ($\sqrt{s_{NN}} = 86.6$ GeV) in (c) and (d); and $p+$Ar ($\sqrt{s_{NN}} = 110.4$ GeV) in (e) and (f). The black curves are the $p+A$ calculations. The colored curves (solid and dashed) show the QCD $p+p$ calculations (no IC). The $p+A$ rapidity distributions are shown for EPPS16 only (solid) and EPPS16 with $P^0_{\mathrm{ic}\,5} = 1\%$ (dashed). The p_T distributions show EPPS16 only (solid); EPPS16 with k_T kick (dashed); EPPS16 and $P^0_{\mathrm{ic}\,5} = 1\%$ (dot-dashed); and EPPS16, k_T kick and $P^0_{\mathrm{ic}\,5} = 1\%$ (dotted). The $p+$Ne data are from arXiv:2211.11633; the $p+$He and $p+$Ar data are from PRL **122**, 132002 (2019).

SMOG J/ψ Results Compared to Calculations

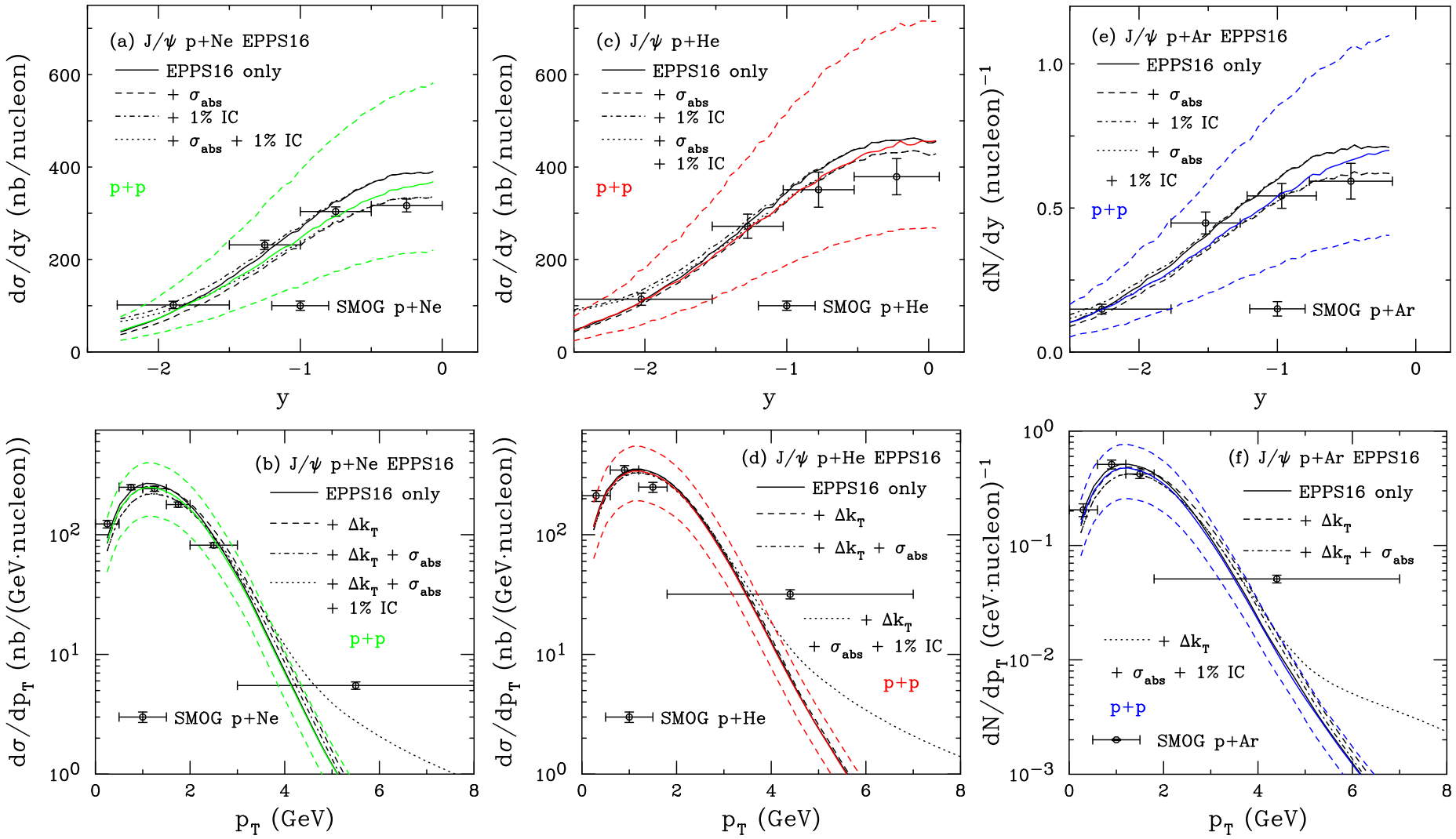

Figure 12: The J/ψ cross section as a function of y in (a), (c), (e) and p_T in (b), (d), (f) for p+Ne ($\sqrt{s_{NN}} = 68.5$ GeV) in (a) and (b); p+He ($\sqrt{s_{NN}} = 86.6$ GeV) in (c) and (d); and $p + $ Ar ($\sqrt{s_{NN}} = 110.4$ GeV) in (e) and (f). The black curves are the $p + A$ calculations. The colored curves (solid and dashed) show the CEM $p + p$ calculations (no IC). The $p + A$ rapidity distributions are shown for EPPS16 only (solid); EPPS16 with absorption (dashed); EPPS16 and $P^0_{\rm ic\,5} = 1\%$ (dot-dashed); and EPPS16, absorption, and $P^0_{\rm ic\,5} = 1\%$ (dotted). The p_T distributions show EPPS16 only (solid); EPPS16 with k_T kick (dashed); EPPS16, absorption, and k_T kick (dot-dashed); and EPPS16, absorption, k_T kick and $P^0_{\rm ic\,5} = 1\%$ (dotted). The $p + $ Ne data are from arXiv:2211.11645; the $p + $ He and $p + $ Ar data are from PRL **122**, 132002 (2019).

Charm Tetraquark Production by Intrinsic Charm

Calculated charm tetraquarks with 1, 2 or 4 charm or anticharm quarks with up to 9 particle states

States that can be described as pairs of heavy flavor mesons like $X(3872) \equiv D\overline{D}$ and $X_s \equiv D_s\overline{D}_s$ whereas tetraquark candidates such as $T_{\psi s}(c\overline{c}s\overline{q})$ and $T_{cs0}(c\overline{s}q\overline{q}')$ will not form a mass peak unless the state is assumed to be four independent partons

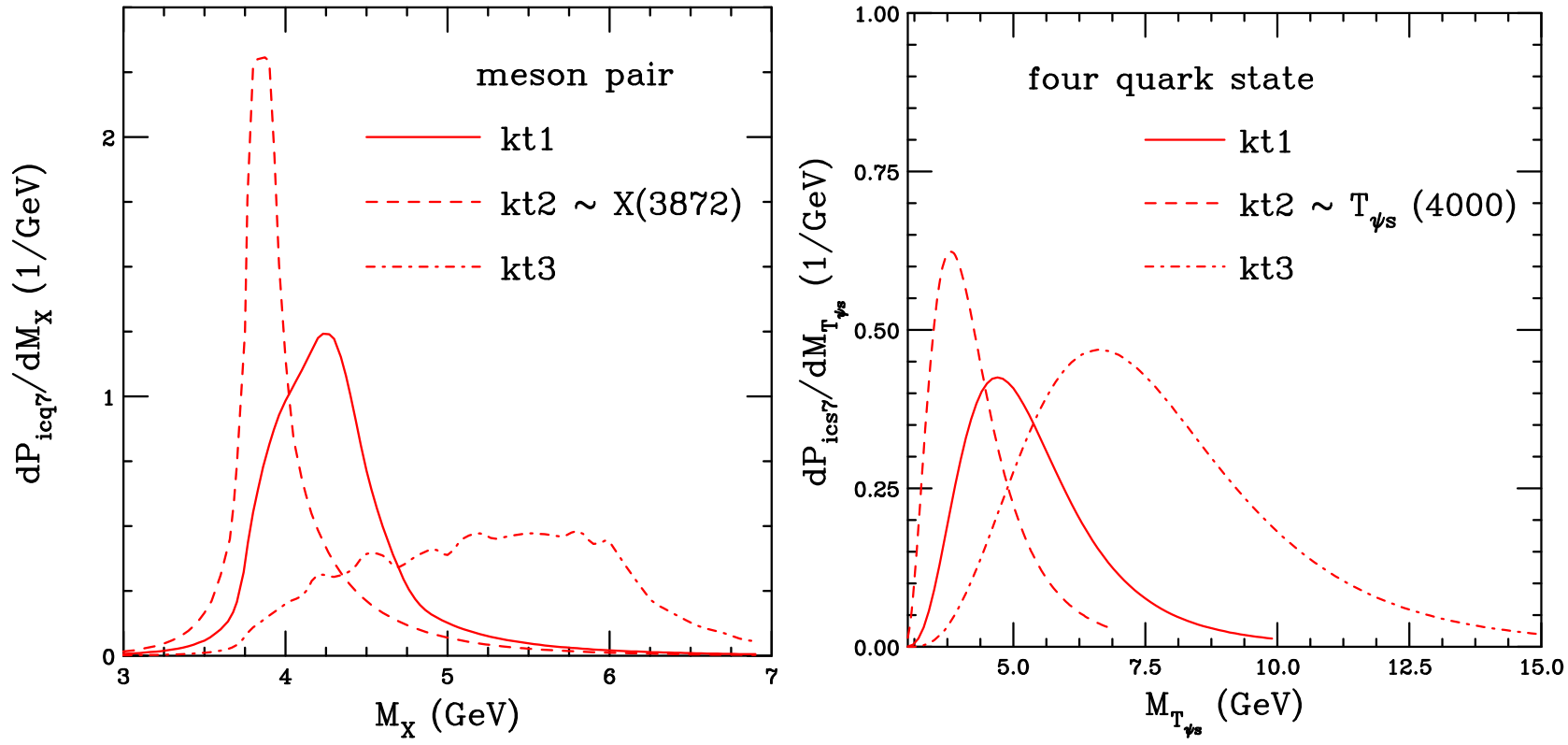

Figure 13: (Left) The $X(3872)$ probability distribution, calculated assuming that the X is a bound meson pair as a function of mass of the state. (Right) The $T_{\psi s}$ probability distribution, calculated assuming as a function of mass of the state. Calculations are nade for different assumptions of the k_T integration range. (RV, arXiv:2405.09018.)

How Important is This at the LHC?

The improved color evaporation model can describe the LHCb data very well without intrinsic charm (IC on the plot)

The small intrinsic charm contribution at high p_T is not surprising based on the rapidity distributions (right), the rapidity range of the LHCb data captures only about 0.1% of the intrinsic charm distribution at 13 TeV

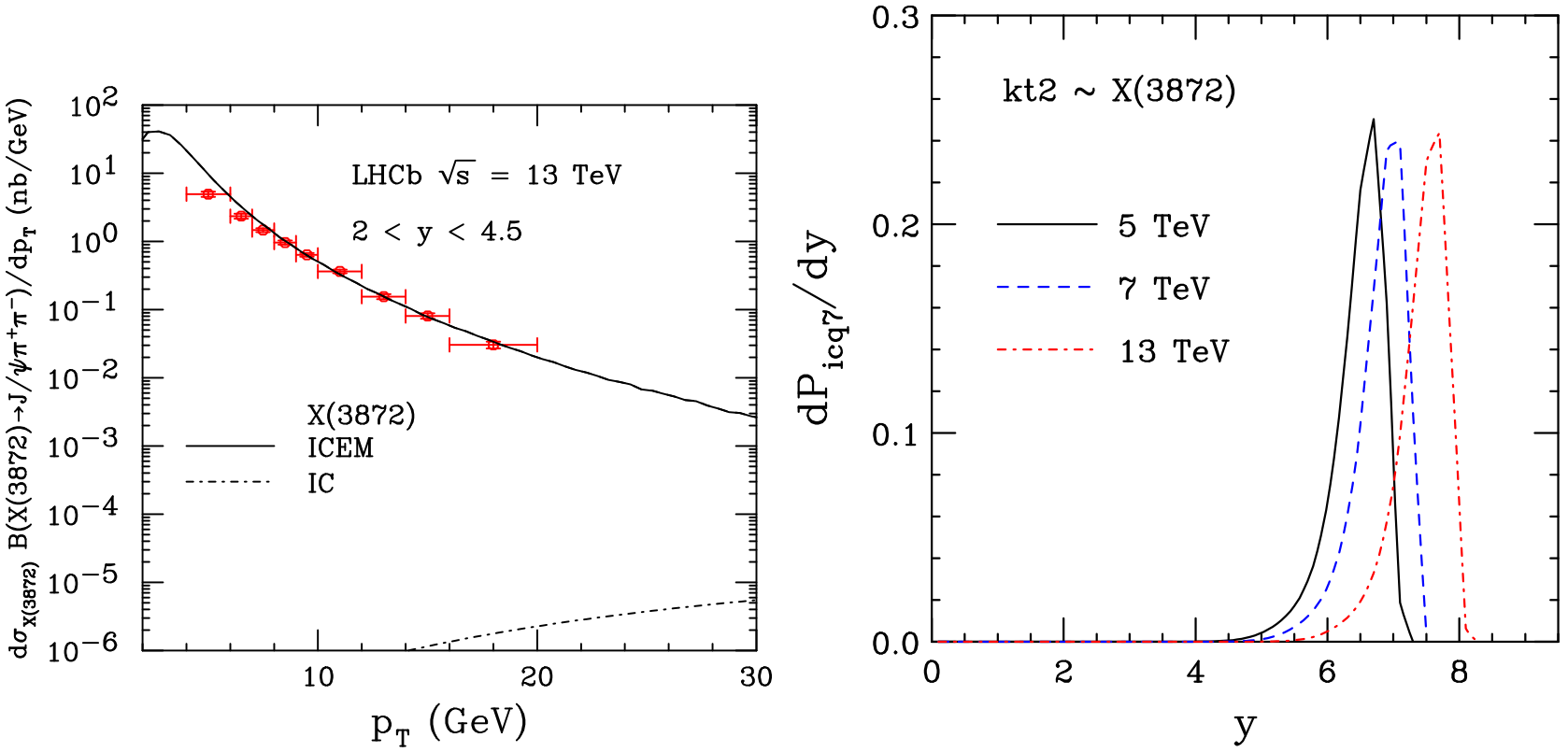

Figure 14: (Left) The $X(3872)$ p_T distribution from the ICEM (solid) and intrinsic charm (dot-dashed) contributions at $\sqrt{s} = 13$ TeV in the rapidity interval $2 < y < 4.5$, The $X(3872)$ rapidity distributions from intrinsic charm at 5, 7 and 13 TeV. (RV, arXiv:2405.09018.)

Summary

Open heavy flavor production is well under control

Quarkonium production can be described by NRQCD and ICEM approaches; NRQCD still has issues describing all production processes while ICEM calculations are venturing into processes beyond hadroproduction

Intrinsic charm, new in the 1980's is experiencing a renaissance of new interest

Model calculations in good agreement with the SMOG $p+A$ cross section data but underestimates asymmetry; more precise data needed at backward rapidity and high p_T

More fixed-target data, from SMOG, NA60+, and elesewhere will add to the overall production picture

Charm measurements at the EIC, to be built at Brookhaven National Lab in the US, will provide new heavy flavor data with proton and ion beams in the future

Intrinsic charm-like states could be used to study exotic hadron production, can distinguish between types of internal tetraquark structure

While not mentioned here, J/ψ measurements have also been used to study internal pressure of the proton via gravitational form factors

Lots of new and exciting opportunities for heavy flavor production in the future

Thank You!